

Piezoelectric and mechanical properties of $\text{Pb}(\text{Zr}_{0.52}\text{Ti}_{0.48})\text{O}_3\text{--Pb}(\text{Y}_{2/3}\text{W}_{1/3})\text{O}_3$ (PZT–PYW) ceramics

SEOK-JIN YOON, JONG H. MOON*, HYUN-JAI KIM

*Division of Ceramics, Korea Institute of Science and Technology and *Department of Inorganic Materials Engineering, College of Engineering, Chonnam National University, Kwang-Joo 500-757, Republic of Korea*

The piezoelectric and mechanical properties of hot-pressed PZT–PYW were investigated. As the $\text{Pb}(\text{Y}_{2/3}\text{W}_{1/3})\text{O}_3$ concentration increased, the piezoelectric constant (d_{33}) also increased up to a concentration of 3 mol % PYW reaching a value of $485 \times 10^{-12} \text{ CN}^{-1}$, but beyond this concentration it continuously fell. A decrease in grain size with increasing $\text{Pb}(\text{Y}_{2/3}\text{W}_{1/3})\text{O}_3$ content in the system changed the transgranular fracture mode to an intergranular fracture mode, resulting in an enhancement in K_{1c} from $0.83 \text{ MPam}^{1/2}$ at 1 mol % PYW to $1.1 \text{ MPam}^{1/2}$ at 3 mol % PYW. Consequently, the highest d_{33} and K_{1c} values were obtained at the composition $0.97\text{Pb}(\text{Zr}_{0.52}\text{Ti}_{0.48})\text{O}_3\text{--}0.03\text{Pb}(\text{Y}_{2/3}\text{W}_{1/3})\text{O}_3$.

1. Introduction

The mechanical properties of piezoelectric ceramics are very important in determining their application in piezoelectric components. A number of studies have been carried out on the mechanical properties of the Lead Zirconate Titanate ($\text{Pb}(\text{Zr,Ti})\text{O}_3$) system [1, 2]. Unfortunately, the fracture toughness (K_{1c}), which represents the resistance to crack propagation, of PZT ceramics has its lowest value at the composition corresponding to the morphotropic phase boundary (MPB) at which the best piezoelectric properties are obtained [3].

The toughening mechanism that applies in PZT has been suggested to be domain switching (twinning) and microcracking within the stress field of propagating cracks, by Pohanka *et al.* [4] whilst Freiman *et al.* [5] have proposed a phase transformation. However, these toughening mechanisms are intrinsic properties which are determined as a function of composition, thus it is difficult to control the toughening mechanisms in order to enhance fracture toughness in the MPB region of PZT ceramics. Therefore, other processing techniques are needed to improve the fracture toughness in this region.

In the present paper, $\text{Pb}(\text{Y}_{2/3}\text{W}_{1/3})\text{O}_3$ (PYW) is added to $\text{Pb}(\text{Zr}_{0.52}\text{Ti}_{0.48})\text{O}_3$ in order to improve the piezoelectric properties of the system, and also to enhance the mechanical properties by controlling the microstructure and fracture mode of the PZT.

2. Experimental procedure

Reagent grade PbO , ZrO_2 , TiO_2 , Y_2O_3 and WO_3 were used as the starting materials. Chosen compositions were mixed for 12 h with zirconia balls as the grinding media and deionized water as the lubricant. The mixed powders were dried in an oven and calcined at 850°C for 1 h. The resulting powders were sintered at 1200°C for 1 h under a pressure of 20 MPa in order to eliminate pores. The sintered pellets devoid of pores were ground to a 1 mm thickness and electroded using silver paste. The electroded samples were poled at 100°C using 35 kV cm^{-1} for 30 min in silicon oil. The piezoelectric properties were measured 24 h after the poling. A low frequency impedance analyser (HP4192A) was used for measuring the dielectric constant (K_{33}^T) and the low ($\tan \delta$) at 1 kHz. The piezoelectric constant was measured using the d_{33} meter by Channel Products Inc. A network analyser (HP3577A) was used for the measurement of the frequency responses.

The fracture toughness values were determined using an indentation–fracture method [6]. For this purpose, sintered specimens were cut, ground by SiC grinding paper, and polished with fine diamond paste. Vickers diamond pyramid indentations (Vickers indenter, Dia Tester 2RC, 310-136/10196; Amsler Otto Wolpert-Werke GmbH, Germany) were then made on polished specimens using a 2.94 N indentation load. The holding time after an indent was 10 s. The data

*Author to whom correspondence should be addressed

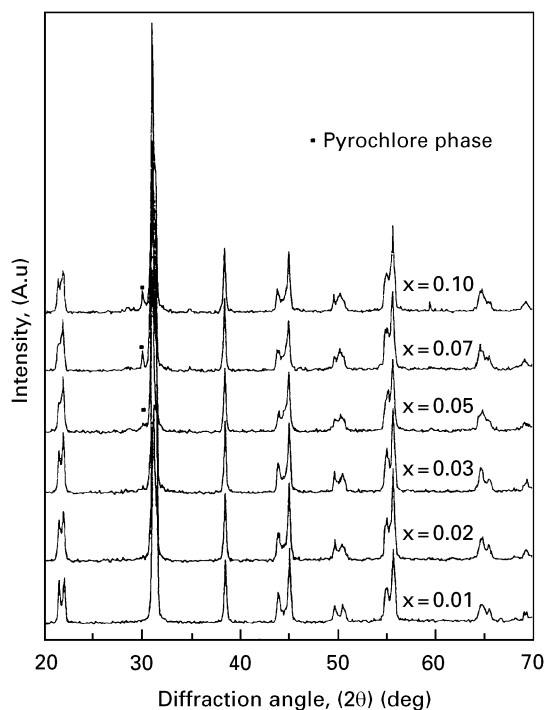


Figure 1 X-ray diffraction patterns for xPZT-(1-x)PYW specimens sintered at 1200 °C for 1 h under a 20 MPa pressure.

TABLE I Lattice parameters and c/a ratio as a function of $\text{Pb}(\text{Y}_{2/3}\text{W}_{1/3})\text{O}_3$ content

Mol %	Lattice parameter		Tetragonality c/a
	a(nm)	c(nm)	
1	0.40216	0.41224	1.0251
2	0.40220	0.41260	1.0259
3	0.40232	0.41301	1.0267
5	0.40250	0.41318	1.0265
7	0.40238	0.41290	1.0264
10	0.40194	0.41238	1.0260

were obtained using at least five indentations on each specimen. The K_{1c} values were then estimated by measuring the crack length and applying the analysis of Lawn and Fuller [7].

3. Results and discussion

Fig. 1 shows the X-ray diffraction patterns of the specimens sintered at 1200 °C for 1 h under a pressure of 20 MPa. The lattice parameters of those specimens and the c/a ratio are given in Table I. Only the tetragonal phase is present in the composition with 1 mol % PYW. As the amount of PYW increases the c/a ratio of the tetragonal phase increases and a rhombohedral phase is observed. This result is different from the usually observed phenomena in the PZT system that the c/a ratio decreases with increasing rhombohedral phase concentration.

A second phase pyrochlore structured material begins to appear at 5 mol % PYW, the EDAX signals from this phase show that it is a Y, Zr-rich phase. It should be noted that whilst the second phase is detected

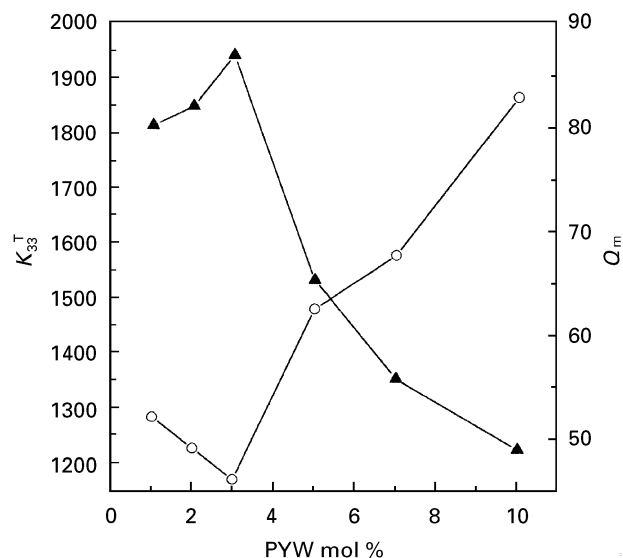


Figure 2 The (▲) dielectric properties and (○) mechanical quality factor as a function of $\text{Pb}(\text{Y}_{2/3}\text{W}_{1/3})\text{O}_3$ content.

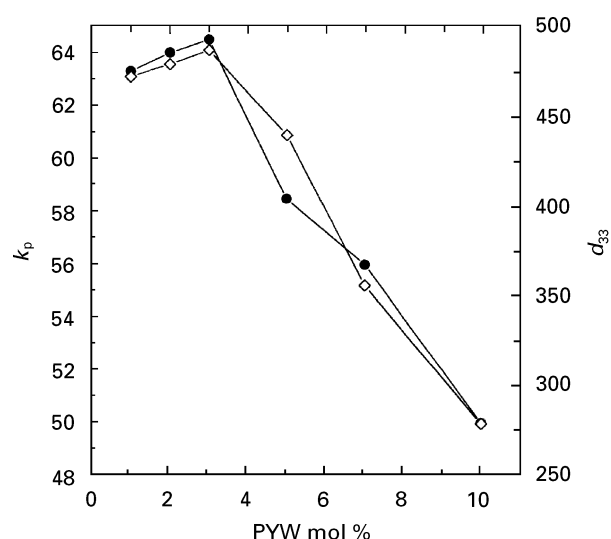


Figure 3 The (◇) piezoelectric properties and (●) the electromechanical coupling factor as a function of $\text{Pb}(\text{Y}_{2/3}\text{W}_{1/3})\text{O}_3$ content.

at 5 mol % PYW by X-ray diffraction, SEM observations clearly show that some second phase particles exist at 1 mol % PYW. This compositional difference is attributed to the point that XRD has a detection unit of area 5 mol % in multiphase systems.

Figs 2 and 3 show the values of the dielectric and piezoelectric properties as a function of PYW content. The dielectric constant (K_{33}^T) linearly decreases with increasing addition of PYW to PZT. The electromechanical coupling factor (k_p) is constant to 3 mol % PYW and is then rapidly degraded at concentrations beyond this level. The value of d_{33} increased up to 3 mol % PYW reaching a maximum value of $485 \times 10^{-12} \text{ CN}^{-1}$, and thereafter declined rapidly. On the other hand, the mechanical quality factor (Q_m) decreased slightly on the addition of 3 mol % PYW, and gradually increased with further increase in the PYW content, reaching a value of 83 at 10 mol % PYW.

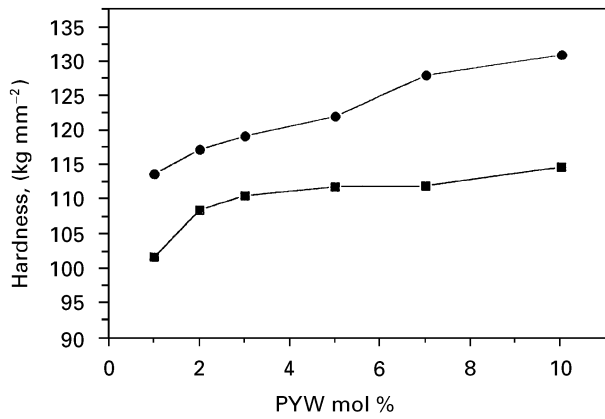


Figure 4 The variation of hardness as a function of $\text{Pb}(\text{Y}_{2/3}\text{W}_{1/3})\text{O}_3$ content for (■) unpoled and (●) poled samples.

The enhancement of K_{33}^T , d_{33} and k_p up to 3 mol % PYW is attributed to the high dipole moment produced as a consequence of the increase in the ratio c/a (Table I) and the formation of A-site vacancies in the perovskite structure created by the introduction of PYW into $\text{Pb}(\text{Zr}_{0.52}\text{Ti}_{0.48})\text{O}_3$. As mentioned previously, the second phase formed by the addition of PYW was a Y, Zr-rich phase. This means that the large Y ion (Ionic radius = 0.089 nm) does not substitute for Zr (ionic radius = 0.061 nm) or Ti (ionic radius = 0.072 nm). Instead W^{6+} ions mainly substitute for the Zr due to a similar ionic radius. This substitution is accompanied by the formation of V_{pp}'' by $\text{W}_{\text{Zr}^{+2}}^{6+} = \text{W}_{\text{Zr}^{00}} + V_{pb}''$ which results in the easy motion of domain walls thereby enhancing K_{33}^T , d_{33} and k_p . The decrease in the c/a ratio and the increase in concentration of the second phase with antiferroelectric properties over 3 mol % PYW degrade the values of K_{33}^T , d_{33} and k_p , but enhance Q_m .

Fig. 4 shows the change in hardness as a function of PYW content. The hardness continuously increases with increasing PYW content. Generally, the tetragonal phase is harder than the rhombohedral phase due to a high chemical bonding energy, so the hardness increases with increasing tetragonality (c/a) and decreasing concentration of the rhombohedral phase. However it has been shown that the amount of rhombohedral phase, the (c/a) ratio and the amount of the second phase increase simultaneously with increasing addition of PYW to the system. In spite of the fact that the amount of rhombohedral phase with a lower bonding energy compared to the tetragonal phase, is increased and the (c/a) ratio is also increased over 5 mol % PYW, the enhancement in the hardness seems to be caused by the second phase having a higher bonding energy than either the tetragonal or rhombohedral phases. The increase in hardness in the poled specimens is known to be due to the alignment of domains by the electric field [2].

Fig. 5 shows the change in the fracture toughness (K_{1c}) in unpoled specimens as a function of PYW concentration. It is found that K_{1c} rises considerably up to 3 mol % PYW and then declines slightly at 5 mol % PYW, and thereafter remains constant. The K_{1c} values of the poled specimens are higher than that

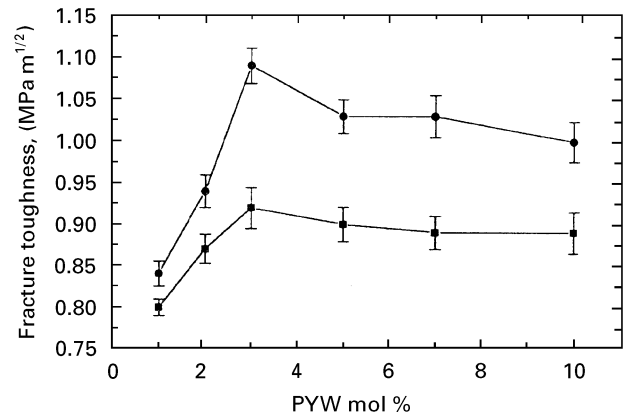


Figure 5 The variation of the fracture toughness as a function of $\text{Pb}(\text{Y}_{2/3}\text{W}_{1/3})\text{O}_3$, for (■) unpoled and (●) poled specimens.

of the unpoled specimens at all compositions. The general trend of the K_{1c} variation in the poled specimens is similar to that of unpoled specimens, but the difference in K_{1c} between unpoled specimens and poled specimens in each composition gradually increases with increasing PYW concentration. The crack lengths were observed to be shorter in the direction of the poling direction compared to the orthogonal direction. The difference in crack sizes has been explained on the basis of domain switching during crack growth.

Fig. 6 shows a scanning electron micrograph, of a propagated crack under microindent, in the specimens containing (a) 1 mol % PYW and (b) 3 mol % PYW. The average grain size of the specimen with 1 mol % PYW was 12 μm and its fracture mode was mainly transgranular, which results in a smooth fracture surface. As the addition of PYW to the system was increased, the average grain size was decreased to 4.5 μm at 3 mol % PYW, and the fracture mode of this specimen was primarily intergranular.

Fig. 7 shows the correlation between the number of grains with intergranular fracture versus the fracture toughness (K_{1c}) in poled and unpoled specimens. As the fraction of intergranular fractured grains increased, the fracture toughness was concurrently enhanced. The increase in intergranular grains in the electrically poled specimen is attributed to the internal stress which was enhanced by the ferroelectric domain alignment at grain boundaries, thereby forming microcracks and resulting in improved fracture toughness. This means that a change in fracture mode is more effective in increasing fracture toughness in the MPB region of PZT than any change in toughening mechanism. It is possible that the toughening mechanism is changed with increasing PYW addition to the system since the grain size decreased and the second phase and rhombohedral phase concentrations increased.

The fracture mode of ceramics is strongly dependent on the grain size. In the present PZT–PYW system, the segregation of the second phase at the grain boundaries with increasing addition of PYW suppress grain growth in the matrix phase and induces the transformation of transgranular to intergranular

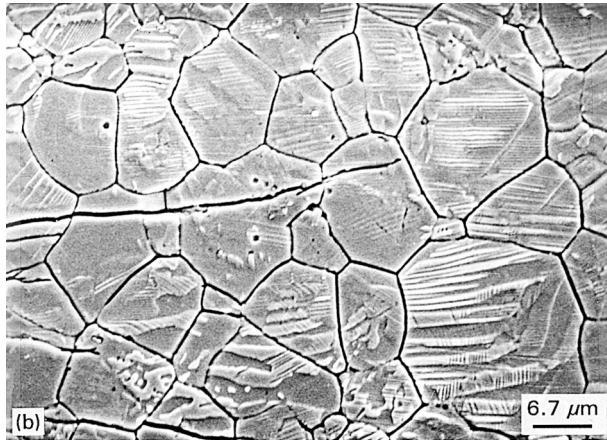
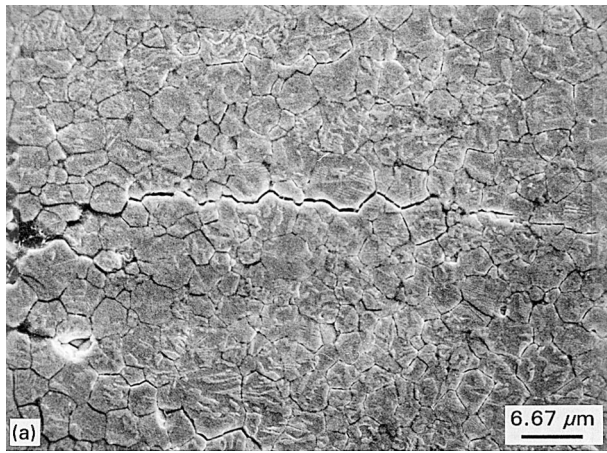


Figure 6 The scanning electron micrograph of the indented specimens at the addition of (a) 3 mol % $\text{Pb}(\text{Y}_{2/3}\text{W}_{1/3})\text{O}_3$ (b) 1 mol % $\text{Pb}(\text{Y}_{2/3}\text{W}_{1/3})\text{O}_3$.

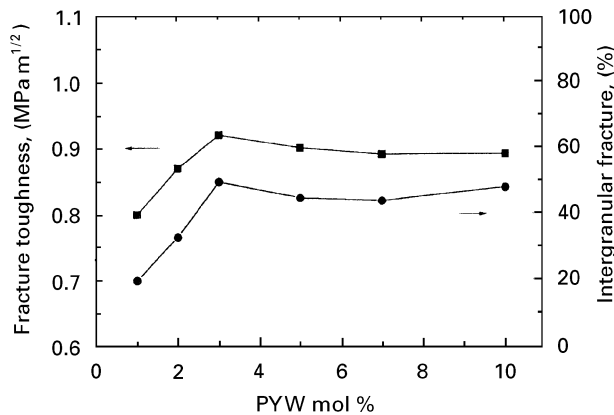


Figure 7 The correlation of the fraction of intergranular fractured grains with the fracture toughness of unpoled specimens.

fracture mode at less than a critical grain size. Kim *et al.* [8] have reported on the relationship between grain size and fracture mode. They note that an inter-

nal stress builds up at grain boundaries during cooling and that this results in intergranular propagation of cracks at small grain sizes and that a release of the internal stress by the formation of ferroelectric polydomain can give rise to transgranular fracture.

The results of this experiment agree with the suggestion that the cracks propagate intergranularly in the poled specimen, although transgranular fracture is dominant before poling. The most significant result from the measurement of the piezoelectric properties and the fracture toughness in the PZT–PYW system is that d_{33} and K_{1c} values were increased to $480 \times 10^{-12} \text{ CN}^{-1}$, and $1.1 \text{ MPa m}^{1/2}$, respectively at 3 mol % PYW.

4. Conclusion

In the PZT–PYW system, the piezoelectric and mechanical properties were investigated. The dielectric constant (K_{33}^1) and piezoelectric constant (d_{33}) were increased up to a 3 mol % PYW content. The fracture toughness (K_{1c}) was also increased up to a 3 mol % PYW content, the increase was in proportion to the fraction of intergranular grains, which was in turn increased by the amount of second phase segregated at grain boundaries. In addition the matrix grain size became smaller with increasing PYW content.

As a consequence, the addition of PYW to PZT affected the defect chemistry and grain size, which resulted in a change in the fracture mode of the system, giving rise to the highest d_{33} and K_{1c} values at 3 mol % PYW.

References

1. K. MEHTA and A. V. VIRKAR, *J. Amer. Ceram. Soc.* **73** (1990) 567.
2. S. S. CHIANG, R. M. FULARTH and J. A. PASK, *J. Amer. Ceram. Soc., Com. Amer. Ceram. Soc.* (1981) C-141.
3. R. C. POHANKA, S. W. FREIMAN, K. OKAZAKI and S. TASHIRO, in "Fracture Mechanics of Ceramics, Vol. 5", edited by R. C. Bradt, A. G. Evans, D. P. H. Hasselman and F. F. Lange (Plenum Press, New York, 1983) p. 353.
4. R. C. POHANKA, S. W. FREIMAN and R. W. RICE, *Ferroelectrics*, **28** (1980) 337.
5. S. W. FREIMAN and J. J. MECHOLSKY, in "Fracture Mechanics in of Ceramics, Vol. 8", edited by R. G. Bradt, D. P. H. Hasselman, and F. F. Lange (Plenum Press, New York, 1985) p. 176.
6. A. G. EVANS and E. A. CHARLES, *J. Amer. Ceram. Soc.* **59** (1976) 371.
7. B. R. LAWN and E. R. FULLER, *J. Mater. Sci.* **10** (1975) 2016.
8. SANG-BEOM KIM, DOH-YEON KIM, JEONG-JOO KIM and SANG-HEE CHO, *J. Amer. Ceram. Soc.* **73** (1990) 161.

Received 6 March
and accepted 1 December 1995